Aerosol Science and Technology

ISSN: 0278-6826 (Print) 1521-7388 (Online) Journal homepage: https://www.tandfonline.com/loi/uast20

Production of neutral molecular clusters by controlled neutralization of mobility standards

G. Steiner, A. Franchin, J. Kangasluoma, V.-M. Kerminen, M. Kulmala & T. Petäjä

To cite this article: G. Steiner, A. Franchin, J. Kangasluoma, V.-M. Kerminen, M. Kulmala & T. Petäjä (2017) Production of neutral molecular clusters by controlled neutralization of mobility standards, Aerosol Science and Technology, 51:8, 946-955, DOI: 10.1080/02786826.2017.1328103

To link to this article: https://doi.org/10.1080/02786826.2017.1328103

Accepted author version posted online: 08 May 2017.
Published online: 26 May 2017.

Article views: 582

AEROSOL SCIENCE AND TECHNOLOGY
2017, VOL. 51, NO. 8, 946–955
https://doi.org/10.1080/02786826.2017.1328103

Production of neutral molecular clusters by controlled neutralization of mobility standards

G. Steiner[a,b], A. Franchin[c,d,e], J. Kangasluoma[c], V.-M. Kerminen[c], M. Kulmala[c], and T. Petäjä[c]

[a]Institute for Ion Physics and Applied Physics, University of Innsbruck, Innsbruck, Austria; [b]Faculty of Physics, University of Vienna, Wien, Austria; [c]Department of Physics, University of Helsinki, Helsinki, Finland; [d]Cooperative Institute for Research in Environmental Sciences (CIRES), University of Colorado, Boulder, Colorado, USA; [e]National Oceanic and Atmospheric Administration (NOAA), Earth System Research Laboratory, Chemical Sciences Division, Boulder, Colorado, USA

ABSTRACT

Measuring aerosols and molecular clusters below the 3 nm size limit is essential to increase our understanding of new particle formation. Instruments for the detection of sub-3 nm aerosols and clusters exist and need to be carefully calibrated and characterized. So far calibrations and laboratory tests have been carried out using mainly electrically charged aerosols, as they are easier to handle experimentally. However, the charging state of the cluster is an important variable to take into account. Furthermore, instrument characterization performed with charged aerosols could be biased, preventing a correct interpretation of data when electrically neutral sub-3 nm aerosols are involved. This article presents the first steps to generate electrically neutral molecular clusters as standards for calibration. We show two methods: One based on the neutralization of well-known molecular clusters (mobility standards) by ions generated in a switchable aerosol neutralizer. The second is based on the controlled neutralization of mobility standards with mobility standards of opposite polarity in a recombination cell. We highlight the challenges of these two techniques and, where possible, point out solutions. In addition, we give an outlook on the next steps toward generating well-defined neutral molecular clusters with a known chemical composition and concentration.

ARTICLE HISTORY
Received 16 July 2016
Accepted 4 April 2017

EDITOR
Jing Wang

1. Introduction

Formation of new atmospheric aerosol particles enhances concentrations of cloud condensation nuclei in the global atmosphere, having a potential to affect clouds' properties and Earth's climate system (Merikanto et al. 2009; Kazil et al. 2010; IPCC 2013). The first steps of new particle formation are taking place at the molecular level, usually below the detection limit of traditional aerosol instrumentation (about 3 nm). The ability to measure aerosol particles and molecular clusters at sizes below 3 nm is therefore crucial for our understanding of the fundamental mechanisms governing atmospheric new particle formation.

Although already possible since several decades (see also Section S1 in the online supplemental information [SI]), the development of instrumentation for the detection of particles in the size range below 3 nm has lately again been pushed forward. (Kulmala et al. 2007, 2013). Current instruments measuring sub-3 nm aerosols and clusters use different working principles, and can be divided into (1) instruments based on electrical mobility analysis like the NAIS (Neutral Clusters and Air Ion Spectrometer; Manninen et al. 2010), (2) high-resolution mass spectrometers with (Jokinen et al. 2012) and without (Junninen et al. 2011) chemical ionization inlets, and (3) new types of condensation particle counters (Stolzenburg and McMurry 1991; Iida et al. 2009; Vanhanen et al. 2011; Kuang et al. 2012). The response of all these new instruments is highly dependent on the charging state and chemical composition of the detected particles and clusters (Kangasluoma et al. 2014). For this reason, these instruments need to be carefully characterized using adequate calibration test aerosols. Since the introduction of the so-called "mobility standards" in 1996 (Rosell-Llombart et al. 1996), generating calibration clusters in the sub-3 nm size range that are electrically

CONTACT G. Steiner gerhard.steiner@uibk.ac.at Institute for Ion Physics and Applied Physics, University of Innsbruck, Technikerstrasse 25, Innsbruck 6020, Austria; or A. Franchin alessandro.franchin@noaa.gov NOAA ESRL Chemical Sciences Division, 325 Broadway, R/CSD2, Boulder, CO 80305, USA.

Supplemental data for this article can be accessed on the publisher's website.

charged has been a standard procedure. Generating electrically neutral calibration clusters, of known chemical composition and number concentration, is experimentally much more challenging. So far, no adequate source for neutral clusters of known chemical composition and number concentration exists.

Our work tackles this problem and focuses on the generation of neutral molecular clusters, taking steps toward producing clusters of well-known chemical composition and concentration, with the long-term goal of using them for calibration.

2. Methods

For the generation of molecular clusters in the size range below 3 nm, a large variety of generation techniques is possible. These techniques range from condensation-evaporation methods over electrospray ionization sources to the generation of monoterpene ozonolysis products in a flow tube (Kangasluoma et al. 2013, 2014). The cluster generation technique chosen in this study is based on electrospray ionization.

2.1. Generation of charged clusters

In this work, we generated charged molecular clusters by electrospray. A short overview on the history of this technique is given in Section S1 of the SI. For our experiments, we used the ionic liquid methyl-trioctylammonium bis (trifluoromethylsulfonyl) imide ($C_{27}H_{54}F_6N_2O_4S_2$, CAS 375395-33-8, melting point −50°C, molar mass 648.55 g/mol, density 1.11 g/cm^3), further on referred to as MTOA-BF3I. The MTOA-BF3I was used at molar concentrations of about 7 mmol/L, using acetonitrile as a solvent (i.e., one drop of MTOA-BF3I with a diameter of 2 mm from a 1 mm diameter pipette tip dissolved in 1 mL acetonitrile). The electrosprayed solution was used to produce positive and negative charged nanodrops (Ku and Ferández de la Mora 2009; Larriba et al. 2011) of the form $A^+(AB)_n$ and $B^-(AB)_m$. The electrospray ion sources used in our experiments are custom-built, following the design originally presented by Rosell-Llompart and Fernández de la Mora (1994).

For the classification of the electrospray-generated clusters, two different high-resolution DMAs were used: the Herrmann-DMA and the UDMA. The Herrmann-DMA is one of the most advanced cylindrical high-resolution DMAs and was designed and built in the laboratory of Juan Fernández de la Mora at Yale University. At optimal operating conditions, it reaches a resolving power between 50 and 75 (Gamero-Castaño and Fernández de la Mora 2000; Martínez-Lozano and Fernández de la Mora 2005). Hereafter, we will refer to the resolution R of a DMA following the definition of Flagan (1999). In the current study, the Hermann-DMA was operated at a resolution power of approximately 20 in the size range of interest (see also Kangasluoma et al. 2016a). The UDMA (Steiner et al. 2010) originates from the laboratory of Georg Reischl from the University of Vienna and also achieves a resolution between 15 and 20 in the sub-3 nm size range. The mobility classification characteristics of both DMAs were calibrated using the mobility standard tetraheptylammonium bromide (Ude and Fernández de la Mora 2005).

2.2. Generation of neutral clusters

In the following sections, we will discuss two possible techniques to generate electrically neutral molecular clusters. The first technique (neutralization technique) involves well-defined, electrospray-generated molecular clusters that are neutralized using unipolar ions that originate from a custom built aerosol neutralizer. The second technique (controlled neutralization technique) is based on the recombination of positively and negatively charged mobility standards, generated by two electrospray sources. The charged clusters were of the type $A^+(AB)_n$ and $B^-(AB)_m$ and formed neutral species of the form $(AB)_{n+m+1}$.

2.2.1. Neutralization technique

The first method was a straightforward neutralization approach of initially charged clusters. In these experiments, the Herrmann-DMA classified negatively charged clusters of MTOA-BF3I. The clusters were subsequently drawn through a custom-built, switchable aerosol neutralizer. Cryogenic nitrogen was used as a carrier gas in the electrospray. When the neutralizer was switched off, the cluster mobility spectrum could be recorded with a TSI 3068B aerosol electrometer. When switched on, the neutralized clusters were detected with a diethylene glycol (DEG) based Airmodus Particle Size Magnifier A11 (PSM; Vanhanen et al. 2011), connected to a TSI 3772 condensation particle counter (CPC), using n-butyl alcohol as condensing fluid. An ion precipitator (IP; Kangasluoma et al. 2015) in front of the PSM ensured that the measurements with the PSM were not biased by signals originating from charged clusters. An overview of the experimental setup for the neutralization of electrospray-generated clusters is shown in Figure 1a.

The special feature of this setup is the switchable aerosol neutralizer, the so-called "ion gun" (IG; Figure 1b). It consists of a stainless steel housing for a ^{241}Am radioactive source, producing bipolar ions. An electric field ensures that only ions of one polarity are drawn into a 990 cm^3 (9.9×10^{-4} m^3) stainless steel reaction chamber. A counter flow of 0.2 L/min (3.3×10^{-6} m^3/s)

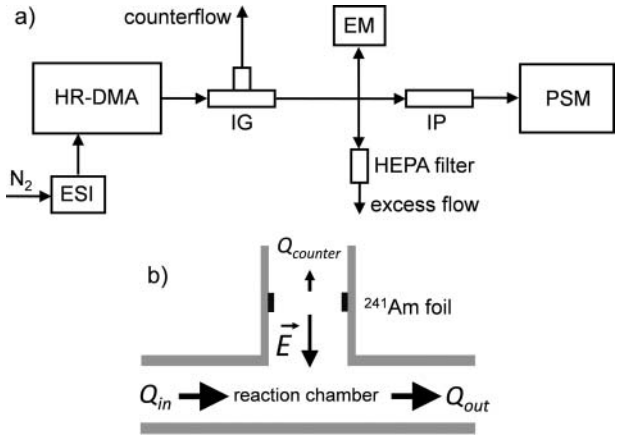

Figure 1. (a) Experimental setup for the neutralization of electrospray-generated mobility standards. ESI (electrospray ion source), HR-DMA (high-resolution DMA), IG (ion gun neutralizer), EM (aerosol electrometer), HEPA (high-efficiency particulate arrestance) filter, IP (ion precipitator), and PSM (particle size magnifier). (b) Schematic view of the ion gun (IG) neutralizer. A ^{241}Am radioactive source produces bipolar ions in the carrier gas. An electric field gradient $\vec{E}$ pulls ions of one polarity into a reaction chamber where the ions can recombine with size-selected clusters originating from the electrospray ion source. A counter flow $Q_{counter}$ of 0.2 L/min (3.3×10^{-6} m^3/s) ensures that the ions of opposite polarity, which are deflected by the electric field, are efficiently drawn into an exhaust line.

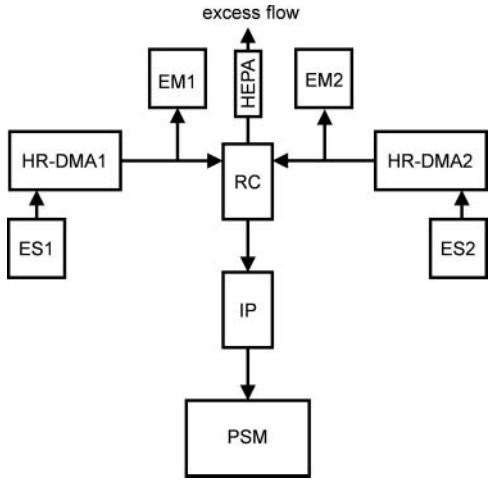

Figure 2. Schematic overview of the experimental setup for the controlled neutralization of well-defined positive and negative electrospray-generated ion clusters. ES1 and HR-DMA1 (UDMA) produce and classify positive ion clusters of a certain size, ES2 and HR-DMA2 (Hermann - DMA) take care of negative polarity ions. EM1 and EM2 are aerosol electrometers, detecting the total number concentration of the classified positive and negative clusters. The airflows containing the positive and negative ion clusters are merged in a recombination cell (RC). An ion precipitator (IP) ensures that no ions obscure the detection of neutral clusters in the particle size magnifier (PSM). The remaining airflow is discarded via a HEPA-filter as excess flow.

ensures that the ions that are deflected by the electric field gradient are transported into an exhaust line. When the ions from the "ion gun" reach the reaction chamber, they recombine with the ion clusters originating from the electrospray source. For a sample inlet air flow of 11 L/min (1.8×10^{-4} m^3/s), the ion-cluster recombination time is on the order of 2.5 s.

2.2.2. Controlled neutralization technique

The neutralization of electrospray-generated clusters presented in Section 2.2.1 bears one major disadvantage: the unknown chemical nature of ions originating from the "ion gun" used for the neutralization. The ion clusters produced by the ionizing radiation do not have a well-defined composition and depend on contaminant trace gases in the carrier gas (Steiner and Reischl 2012; Steiner et al. 2014; Maisser et al. 2015). This drawback can be overcome with an alternative method to generate neutral clusters: the controlled neutralization by the recombination of well-defined ion clusters of positive and negative polarity. For this purpose, two high-resolution DMAs, supplied by two electrospray ion sources, are needed. In our experimental setup, the Herrmann-DMA was used to classify ion clusters of negative polarity. Positively charged ion clusters were classified with the UDMA. To detect the classified positive and negative ion clusters, a TSI 3068B aerosol electrometer, downstream from the Hermann-DMA, and a custom built aerosol electrometer, downstream from the UDMA, were used.

The airflows, transporting positive (6.9 L/min; 1.15×10^{-4} m^3/s) and negative ion clusters (7.9 L/min; 1.32×10^{-4} m^3/s), were merged in a reaction chamber. The reaction chamber had a volume of 29 cm^3 (2.9×10^{-5} m^3). Again, an ion precipitator in front of the PSM ensured that only neutral clusters could enter the instrument for detection. The clusters are drawn through the reaction chamber and subsequently to the ion precipitator, by a volumetric flow rate of 2.5 L/min (4.17 m^3/s), defined by the inlet flow rate of the PSM, leading to a reaction time of $\tau = 0.7$ s. Figure 2 shows the schematics of the setup.

2.3. Detection of neutral clusters

The detection of neutral molecular clusters was carried out with the diethylene glycol (DEG) based Particle Size Magnifier A11 from Airmodus (PSM, Vanhanen et al. 2011).

Like any other CPC, the PSM requires calibration in order to determine its particle detection efficiency. It is known that the detection efficiency is strongly dependent on the size, chemical composition, and charging state of particles (Stolzenburg and McMurry 1991; Winkler et al.

2008; Kangasluoma et al. 2016b). Unfortunately, this dependency causes a crucial impasse: we want to use the PSM as a detector for neutral particles, but we can only obtain clear information on its detection efficiency when using charged particles. In case of the experiments presented here, the PSM detection efficiency was determined by using negatively charged MTOA-BF3I clusters. More details on the detection efficiency of the PSM can be found in Section S2 of the SI. This prevents us from going beyond making estimates for the detection efficiency of neutral clusters. Therefore, the current work must be considered a feasibility study.

2.4. Size of charged and neutral clusters

For molecular clusters, any kind of size definition is ambiguous. Still, the size information of the detected clusters is a desirable quantity to know for quantitative PSM measurements. In the sub 3 nm size range, the mobility equivalent diameter D_{mob} is a widely used quantity, simply because particles and clusters in this size range can be rather easily size segregated and detected by electrical means. Assuming spherical particles, it is rigorously defined by the Stokes–Millikan equation (see the SI, S1). As pointed out by Tammet (1995) and Ku and Fernández de la Mora (2004), this correlation bears at least two limitations: (a) the ignorance of the finite diameter D_{gas} of the carrier gas molecules and (b) no added drag on the particles due to ion dipole interactions. The so far most advanced approximation, taking into account the latter effects, is a modified Stokes–Millikan equation by Fernández-García and Fernández de la Mora (2013, 2014):

$$Z_{mod} = \frac{3}{16} \cdot \frac{i \cdot e_0}{p} \cdot \left(\frac{2 \cdot \pi \cdot k \cdot T}{m_{gas}}\right)^{1/2} \cdot \left(1 + \frac{m_{gas}}{m}\right)^{1/2} \cdot \frac{(1 + f(Kn))(1 - \beta\varepsilon^*)}{\xi_m \cdot \frac{\pi}{4} \cdot \left(D_{mass} + D_{gas}\right)^2}, \quad [1]$$

where e_0 is the elementary charge, ie_0 and m are the charge and mass of the ion, k is Boltzmann's constant, m_{gas}, T and p are the molecular weight, temperature, and pressure of the carrier gas. The factors $f(\mathrm{Kn})$, β, ε^*, and ξ_m are described in the SI, S1. The factor ε^* takes the ion-induced dipole interaction between the charged nanodrops and the polarized neutral carrier gas molecule into account. In this equation, the finite size of the gas molecules is taken into account by augmenting the mobility diameter D_{mob} by the effective gas molecule diameter D_{gas}; $D_{mob} = D_{mass} + D_{gas}$, *where* D_{gas} is found to be 0.26 nm. The mass diameter D_{mass} is defined by Equation (2):

$$\mathrm{m} = \frac{\pi}{6} \cdot \rho \cdot (D_{mass})^3, \quad [2]$$

where m and ρ are the mass and the bulk density (see also Ku and Fernández de la Mora 2004) of the particle/cluster. The mass diameter is often used to describe the "real," physical diameter of an airborne cluster.

The detailed mechanisms describing the ion–ion recombination are still an open questions. For the neutralization experiment using the ion gun ions, we are therefore considering two neutralization pathways that lead to different final sizes: (1) the neutralization happens by charge-transfer during a collision between a charged cluster and an ion of the opposite polarity without the attachment of the discharging species. This would lead to a final cluster with the same size (D_{mass}) as the initial cluster. Since the charge exchange during a collision also includes the transfer of translational energy, this model potentially could promote ion fragmentation, leading to completely different ion species. This fragmentation is not further discussed in this study but its possibility should be kept in mind. Also, similar studies (Gamero-Castaño and Fernández de la Mora 2000; Attoui et al. 2013a,b) have observed that charge-reduced clusters always show lower mobilities than the corresponding pure cluster of that charging state. This indicates that the clusters are discharged by the attachment of gas phase ions, making the product ion somewhat larger and promoting a different mechanism. (2) The neutral cluster is treated as a spherical cluster, the volume of which is the sum of the volumes ($V_1 + V_2$) of the charged cluster and the neutralizing ion, which are both treated as spheres. The diameter D_{vol} of the enlarged cluster is, in this case, calculated according to Equation (3):

$$D_{vol} = \sqrt[3]{6\pi \cdot (V_1 + V_2)}. \quad [3a]$$

$$\text{with } V_{1,2} = \frac{1}{6} \cdot \pi \cdot D_{mass,\ 1,2}. \quad [3b]$$

The calculated diameters are listed in Section 4, Table 1.

It needs to be kept in mind that these cluster diameters are approximated best-estimates, following the current knowledge of mobility–size relationships. For upcoming studies on this topic, the comparison of experimental mobility measurements with model predictions (Mesleh et al. 1996; Shvartsburg et al. 2007; Larriba and Hogan 2013) considering spherical and non-spherical geometries, with and without taking ion dipole interactions into account, will allow a better understanding of

Table 1. Cluster properties in the neutralization experiments. Considering two neutralization pathways (Section 2.4), two different final sizes (D_{mass} and D_{vol}) of the neutralized clusters are listed.

Negative MTOA-BF3I clusters		Positive IG – ions	Neutralized cluster	
			D_{mass}[nm]	D_{vol}[nm]
Monomer	1.80 [cm^2/Vs] 0.84 [nm]	1.14 [cm^2/Vs]	0.84	1.25
Dimer	0.77 [cm^2/Vs] 1.38 [nm]	1.10 [nm]	1.38	1.59
Trimer	0.55 [cm^2/Vs] 1.68 [nm]		1.68	1.82

ion–ion interactions and the final size of recombined clusters.

3. Theoretical methods

In order to model the number concentration of neutral clusters produced from the recombination of ion clusters, we used a simple system of differential equations. The following equation describes the change in time in number concentration of ions or charged clusters:

$$\frac{dN^{\pm}}{dt} = -k_{loss} \cdot N^{\pm} - k_{rec} \cdot N^{+}N^{-}, \quad [4]$$

where $N^{\pm}$ is the number concentration of ions or charged clusters. k_{loss} is the diffusional loss rate of particles onto the walls and k_{rec} is the ion–ion recombination coefficient. The first term on the right-hand side of Equation (4) describes the loss of the ions to the walls and the second term represents the decrease in the number concentration of ionic clusters of opposite polarity due to recombination. The change in the number concentration of neutral clusters N^0 is given by the following equation:

$$\frac{dN^{0}}{dt} = -k_{loss} \cdot N^{0} + k_{rec} \cdot N^{+}N^{-}. \quad [5]$$

The first term on the right-hand side of Equation (5) describes the loss of neutral clusters to the walls and the second term describes the increase in the number concentration of neutral clusters due to recombination. The term k_{loss}, used in Equation (4) for charged clusters, was determined experimentally by comparing the concentrations of monodispersed charged clusters at the beginning and at the end of our setup. For neutral clusters, in Equation (5), we used the same k_{loss} values as in Equation (4) due to experimental limitations. Therefore, we might be overestimating the diffusion losses in Equation (5). Additionally, it should be noted that in our calculations we chose not to include a source term in Equation (4) and a sink term in Equation (5) relative to recharging of neutral clusters. Such probability is three orders of magnitude lower than the recombination probability (López-Yglesias and Flagan 2013) and therefore, can be neglected.

In the model, the decrease in the number concentration of ions or charged clusters during each time step Δt is given by

$$\begin{aligned} N^{+}_{i+1} &= \Delta t \cdot \left(N^{+}_{i} - k_{loss} \cdot N^{+}_{i} - k_{rec} \cdot N^{+}_{i} \cdot N^{-}_{i}\right) \\ N^{-}_{i+1} &= \Delta t \cdot \left(N^{-}_{i} - k_{loss} \cdot N^{-}_{i} - k_{rec} \cdot N^{+}_{i} \cdot N^{-}_{i}\right). \end{aligned} \quad [6]$$

The increase in the neutral cluster concentration is given by

$$N^{0}_{i+1} = \Delta t \cdot \left(N^{0}_{i} - k_{loss} \cdot N^{0}_{i} + k_{rec} \cdot N^{+}_{i} \cdot N^{-}_{i}\right), \quad [7]$$

and the time step is defined by

$$\Delta t = \frac{\tau}{n_{it}}, \quad [8]$$

where τ is the residence time of ionic clusters in the reaction chamber and n_{it} is the number of iterations, designated as 1000 in our calculations. The size-dependent diffusional losses to the walls were determined experimentally. The chosen values for the ion–ion recombination rate ranged from $k_{rec} = 1 \times 10^{-7}$ to 2.5×10^{-6} [cm^3/s] (Biondi 1969; Israël 1970; Franchin et al. 2015).

4. Results

4.1. Experimental results from the neutralization experiments

An illustrative experiment of the neutralization of electrospray generated ion clusters is illustrated in Figures 3 and 4, where the dimer cluster $A^{-}(AB)_1$ of MTOA-BF3I ($Z = 0.77$ cm^2/Vs, $1/Z = 1.30$ V s/cm^2) (Figure 3a) is neutralized by the ions generated in the ion gun (Figure 3b). We want to emphasize once more that the ion cluster species produced in the ion gun are by no means well-defined, and that the ion production is limited by the activity of the ^{241}Am and the presence of trace gases in the carrier gas. The only control we have is to consistently run the setup using the same carrier gas, in order to guarantee the experimental reproducibility.

Figure 4 illustrates the neutralization experiment of the MTOA-BF3I dimer cluster ($Z = 0.77$ cm^2/Vs, $1/Z = 1.30$ V s/cm^2). The experiment starts at $t_0 = 00{:}00$, where the electrospray ion source and the HR-DMA are still switched off (set to 0 V). The PSM and electrometer signals oscillate around a background level.

At t_1 (00:06), the electrospray ion source was switched on and the HR-DMA was set to classify the negative dimer cluster of MTOA-BF3I. Still, the ion gun-

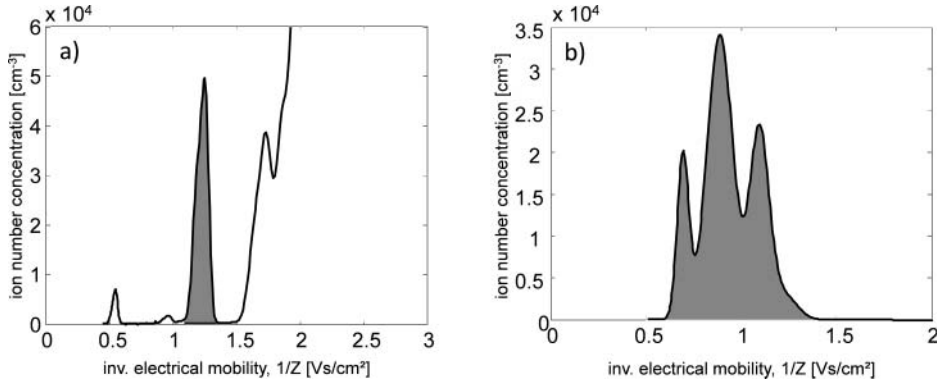

Figure 3. (a) Mobility spectrum of negative MTOA-BF3I clusters. The highlighted peak corresponds to the dimer cluster $A^-(AB)_1$. (b) Mobility spectrum of positive ions produced by the ion gun.

neutralizer remained switched off. Accordingly, no "ion gun ions" entered the reaction chamber to recombine with the MTOA-BF3I clusters. In fact, they were drawn out of the system by the counter flow $Q_{counter}$ (Figure 1b). The classified dimer MTAO-BF3I clusters showed a stable signal level of $4 \times 10^4 \pm 303$ ions/cm^3 in the electrometer and the PSM signal was still at the background level. This also verified the proper operation of the ion precipitator in front of the PSM inlet.

At t_2 (00:14), the ion gun was switched on by applying an electric field that pushed the positive ions against the 0.2 L/min counterflow and into the reaction chamber, where they recombined with the negative dimer MTOA-BF3I. The PSM signal instantaneously rose to a level of 28 ± 6 particles/cm^3 (background corrected). The electrometer signal also rose to an elevated level that originated from an undefined combination of the non-neutralized MTOA-BF3I clusters and the ion gun-ions.

At t_3 (00:54), the electrospray ion source was switched off while keeping the ion gun switched on. This led to a decrease in the PSM signal to the background level, verifying that the PSM signal between t_2 and t_3 originated from neutral recombination products of positive "ion gun ions" and negative MTOA clusters. The increased electrometer signal between t_3 and t_4 is caused by positive ions originating from the ion gun. At t_4 (00:58), the electrospray ion source was switched on again, repeating the neutralization experiment of the dimer cluster. Finally, at t_5 (01:03) the ion gun was switched off again. The PSM signal returned to its background level and the EM signal again showed the stable number concentration of around 4×10^4 particles/cm^3 for the HR-DMA classified negative MTOA-BF3I dimer clusters.

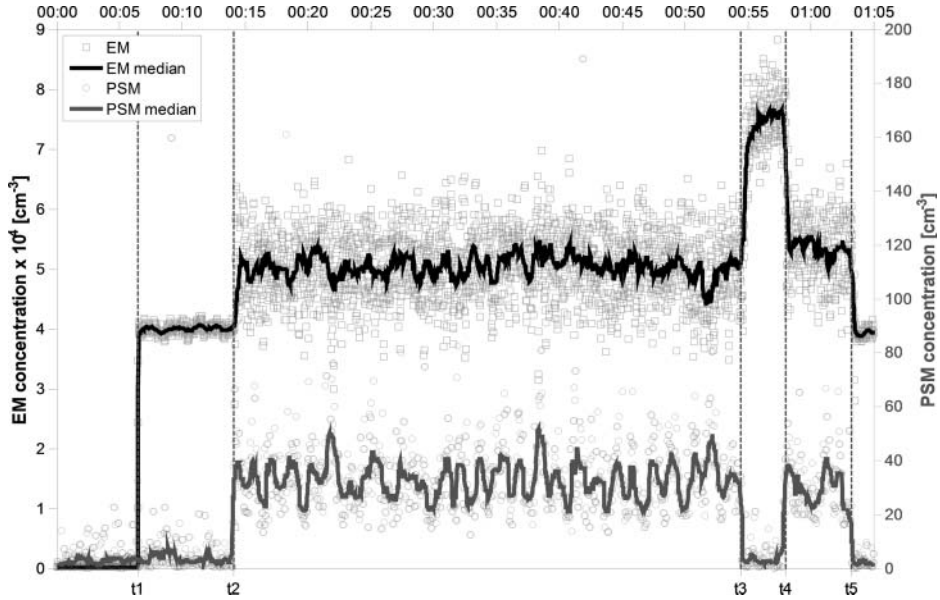

Figure 4. Time series of zero-corrected electrometer and PSM signals during the neutralization experiment of the dimer cluster of MTOA-BF3I.

The same type of experiment, not shown in detail here, was performed for the monomer ($Z = 1.80$ cm^2/V s, $1/Z = 0.56$ V s/cm^2) and trimer ($Z = 0.55$ cm^2/Vs, $1/Z = 1.82$ V s/cm^2) cluster of MTOA-BF3I. The neutralization of the trimer cluster yielded a substantially higher raw neutral cluster number concentration of 1239 ± 90 neutral clusters/cm^3. No successful experiments can be reported for the neutralization of the monomer cluster, most probably due to a poor detection efficiency of the PSM in that size range.

The detected, raw number concentrations of neutral clusters, need to be corrected for the size-dependent detection efficiency of the PSM (see the SI, Section S2). Table 1 summarizes the physical properties of the ion clusters and the estimated sizes of neutralized clusters. The electrical mobility and diameter of the neutralizing ions were determined as a weighted average from the mobility spectrum of the ions. Due to the possible neutralizing pathways, the diameter of the neutralized clusters was determined as D_{mass} and D_{vol}, following Equations (2) and (3) from Section 2.4. Table S1 lists the total measured number concentration of the clusters involved in the neutralization experiments.

4.2. Experimental results from the controlled neutralization experiments

Figure 5 illustrates the recombination experiment of the positive ($Z = 0.62$ cm^2/Vs, $1/Z = 1.61$ V s/cm^2) and negative ($Z = 0.77$ cm^2/Vs, $1/Z = 1.30$ V s/cm^2) dimer clusters of MTOA-BF3I. At the beginning of the experiment t_0, (00:00), HR-DMA 1 already classified the positive dimer cluster of MTOA-BF3I. At this time, HR-DMA 2 (responsible for the classification of the negative clusters) was still switched off and no ions exited the HR-DMA 2. The ion precipitator in front of the PSM ensured that no positive clusters entered the PSM. Accordingly, at the beginning of the experiment, the PSM signal (neutral signal) was at a background level. At t_1 (~00:01), HR-DMA 2 was set to classify the negative dimer of MTOA-BF3I. Instantaneously, also the signal of neutral recombination products rose in the PSM to a (background corrected) level of 88 ± 9 cm^{-3}. These settings were kept for roughly 4 min, while at t_2 (~00:05) HR-DMA 2 was switched off again, resulting in a return of the neutral PSM signal to its prior background level.

Analogously to the neutralization experiment, the number concentration of detected neutral clusters needs to be corrected for the size-dependent detection efficiency of the PSM. Table 2 summarizes the physical properties of the positive and negative MTOA-BF3I clusters, and the estimated size of the neutral recombination products, calculated as D_{vol}, following considerations (3) from Section 2.4. Table S2 lists the total measured number concentration of the clusters involved in the neutralization experiments. The cluster–cluster recombination experiment was carried out with all possible

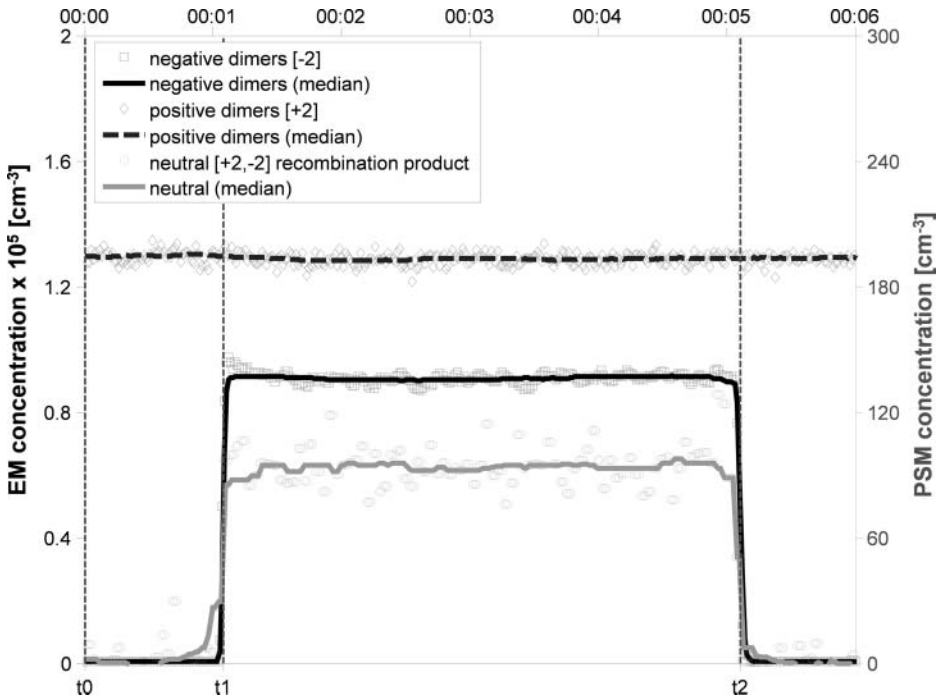

Figure 5. Time series of electrometer ([−2], [+2]) and PSM signals ([+2, −2]) during the controlled neutralization experiment of the positive and negative dimer clusters of the ionic liquid MTOA-BF3I.

Table 2. Cluster properties in the recombination experiments. The size of the recombined, neutral clusters is calculated as D_{vol}, following again the considerations in Section 2.4.

			Positive MTOA-BF3I clusters		
			[+1] 1.00 [cm²/Vs] 1.19 [nm]	[+2] 0.62 [cm²/Vs] 1.57 [nm]	[+3] 0.49 [cm²/Vs] 1.79 [nm]
negative MTOA-BF3I clusters	[−1]	1.80 [cm²/Vs] 0.84 [nm]	1.32	1.64	1.85
	[−2]	0.77 [cm²/Vs] 1.38 [nm]	1.63	1.87	2.03
	[−3]	0.55 [cm²/Vs] 1.68 [nm]	1.86	2.05	2.19

combinations of mixing positive and negative MTOA-BF3I clusters.

4.3. Comparison of experimental data with model results

We compared the measured concentrations from the neutralization experiments and from the controlled neutralization experiments with the modeled results. An example of the output of our model of the concentration of cluster as a function of time is given in Figure S2.

For the comparison (see also Section S3 in the SI), we first solved the set of differential equations for k_{rec} = (0.1; 0.2; 0.5; 0.7; 1.4; 2.0; 2.5) × 10^{-6} [cm^3/s] using the initial concentration of positive and negative ions, N^+_1 and N^-_1, measured with the electrometers (Figure S2). Second, we fitted a power-law function of the type $y = A \cdot x^B$ for each k_{rec}, where y is the final concentration of neutral clusters generated by recombination and x is k_{rec} (Figure S3).

The fitted curves were inverted and used to determine which k_{rec} would determine $N^{0\_model} = N^{0\_measured}$. The results of these calculations are reported in Tables S4 and S5, where the optimal (best) values for k_{rec} are reported with the respective uncertainty calculated as the 68% confidence level (CL) over the fit shown in Figure S3 and summarized in Tables S3 and S4. The optimal k_{rec} coefficients range from 0.19 to 0.75 × 10^{-6} cm^3/s, with the exception for the k_{rec} coefficient related to neutral clusters produced by the negative trimer of MTOA-BF3I and the positive ions generated by the ion gun [−3, +IG]. This k_{rec} lies at much higher value with respect to the others (5.7 × 10^{-6} cm^3/s compared to a mean of 0.46 × 10^{-6} cm^3/s). This suggests that, in this particular case, the $N^{0\_measured}$ could have been overestimated, this could be due to an imperfect classification of the negative MTOA-BF3I due to impurities or multiply charged larger ions. Vice versa, the $N^{0\_measured}$ for all the other cases could have been underestimated, this could be attributed to the fact that one of the biggest uncertainties comes from the PSM detection curve (Figure S1), which is steeper at smaller sizes.

5. Discussion and outlook

In this study, we presented two techniques to generate electrically neutral molecular clusters that may be used for calibration purposes, for novel aerosol instrumentation, and for basic studies at the molecular level. It needs to be emphasized that the measurements presented here should be seen as a feasibility study, since the experimental limitations described still hinder the precise quantification of neutral molecular clusters. The technique of neutralizing well-defined molecular clusters bears the advantage of a simpler setup that can be easily combined with other instrumentation. However, the size and nature of the neutralized clusters are more uncertain, due to the unknown properties of the neutralizing ions. This flaw could be improved for future studies in two ways: first, by using well-defined neutralizing ions, as used in chemical ionization mass spectrometers (CI-MS), and second, by analyzing the neutral products with adequate CI-MS techniques to identify the chemical composition of the new neutral clusters.

The second technique presented here gives more control in terms of the physical and chemical properties of the involved molecular clusters. However, this setup bears the disadvantage of its complexity. In addition, in our study the setup is far from being optimized. The yields of neutral clusters by recombination could be largely improved (1) by redesigning the recombination cell with the aid of computation fluid dynamics (CFD) simulations, and (2) by using high-resolution DMAs that have a better throughput, such as planar DMAs. It is important to note that the increase in transmission has a quadratic dependency on the yield of neutral clusters by recombination (Equation (4)). Therefore, an improvement in transmission from about 1% to, say, 20% (which would be expected using planar DMAs instead of cylindrical ones) would result in a 400-fold increase of ions reaching the recombination chamber. This would mean a theoretical maximum concentration of neutral clusters on the order of 1 × 10^8 cm^{-3}.

The biggest uncertainty in our measurements was the detection efficiency of the PSM with respect to the neutralized or recombined clusters. For future studies, the

PSM detection efficiency needs to be better characterized for a larger variety of clusters, and most importantly for positive, negative, and neutral clusters.

The second largest source of uncertainty is the ion–ion recombination coefficient. In fact, according to the literature, the value of this coefficient can span over one order of magnitude. This large variation is most likely due to the fact that the ion–ion recombination coefficient is not only dependent on physical properties of the participating clusters like size, mass, or electrical mobility, but it is also influenced by ion-chemistry effects. In fact, this method may be used to test various chemical interaction between ions of different chemical composition.

A further improvement in our experiments would involve extending the generated clusters to atmospherically relevant species, such as sulfuric acid, sulfuric acid-amine, and/or ammonia clusters and maybe even to oxidized-organic-compounds. In this way, the method described here could help to investigate neutral molecular clusters of special importance during the process of new particle formation in the atmosphere.

Funding

This work is supported by the Austrian Science Fund, FWF: P27295-N20, the University of Innsbruck promotion grant for young scientists (Project "Cluster Calibration Unit"), the European Commission 7th Framework Programme (Marie Curie Initial Training Network "CLOUD-ITN," Grant 215072), the European Research Council (ERC) Advanced Grant Atmospheric nucleation: from molecular to global scale (ATM-NUCLE) (Grant 227463), and the Academy of Finland via the Centre of Excellence Programme (Projects 1118615 and 272041).

References

Attoui, M., Fernández-Garcia, J., Cuevas, J., Vidal, G., and Fernández de la Mora, J. (2013a). Charge Evaporation from Nanometer Polystyrene Aerosols. *J. Aerosol Sci.*, 55:149–156.

Attoui, M., Paragano, M., Cuevas, J., and Fernández de la Mora, J. (2013b). Tandem DMA Generation of Strictly Monomobile 1-3.5 nm Particle Standards. *Aerosol Sci. Technol.*, 47(5):499–511.

Biondi, M. A. (1969). Atmospheric Electron-Ion and Ion-Ion Recombination Processes. *Can. J. Chem.*, 47(10):1711–1719.

Fernández-García, J., and Fernández de la Mora, J. (2013). Measuring the Effect of Ion-Induced Drift-Gas Polarization on the Electrical Mobilities of Multiply-Charged Ionic Liquid Nanodrops in Air. *J. Am. Soc. Mass Spectrom.*, 24:1872–1889.

Fernández-García, J., and Fernández de la Mora, J. (2014). Electrical Mobilities of Multiply Charged Ionic-Liquid Nanodrops in Air and Carbon Dioxide Over a Wide Temperature Range: Influence of Ion-Induced Dipole Interactions. *Phys. Chem. Chem. Phys.*, 16:20500–20513.

Flagan, R. C. (1999). On Differential Mobility Analyzer Resolution. *Aerosol Sci. Technol.*, 30(6):556–570. doi:10.1080/027868299304417.

Franchin, A., Ehrhart S., Leppä, J., Nieminen, T., Gagné, S., Schobesberger, S., Wimmer, D., Duplissy, J., Riccobono, F., Dunne, E. M., Rondo, L., Downard, A., Bianchi, F., Kupc, A., Tsagkogeorgas, G., Lehtipalo, K., Manninen, H. E., Almeida, J., Amorim, A., Wagner, P. E., Hansel, A., Kirkby, J., Kürten, A., Donahue, N. M., Makhmutov, V., Mathot, S., Metzger, A., Petäjä, T., Schnitzhofer, R., Sipilä, M., Stozhkov, Y., Tomé, A., Kerminen, V.-M., Carslaw, K., Curtius, J., Baltensperger, U., and Kulmala, M. (2015). Experimental Investigation of Ion–Ion Recombination under Atmospheric Conditions. *Atmos. Chem. Phys.*, 15(13):7203–7216. doi:10.5194/acp-15-7203-2015.

Gamero-Castano, M., and Fernández de la Mora, J. (2000). Modulations in the Abundance of Salt Clusters in Electrosprays. *Anal. Chem.*, 72:1426–1429.

Iida, K., Stolzenburg, M. R., and McMurry, P. H. (2009). Effect of Working Fluid on Sub-2 Nm Particle Detection with a Laminar Flow Ultrafine Condensation Particle Counter. *Aerosol Sci. Technol.*, 43(1):81–96. doi:10.1080/02786820802488194.

IPCC. (2013). Climate Change 2013: The Physical Science Basis, in *Contribution of Working Group I to the Fifth Assessment Report of the Intergovernmental Panel on Climate Change*, T. F. Stocker, D. Qin, G.-K. Plattner, M. Tignor, S. K. Allen, J. Boschung, A. Nauels, Y. Xia, V. Bex, and P. M. Midgley, eds., Cambridge University Press, Cambridge, United Kingdom and New York, NY, USA, pp. 1535. doi:10.1017/CBO9781107415324.

Israël, H. (1970). *Atmospheric Electricity: Fundamentals, Conductivity, Ions. Israel Program for Scientific Translations*. U.S. Department of Commerce, National Technical Information Service, Springfield, VA.

Jokinen, T., Sipilä, M., Junninen, H., Ehn, M., Lönn, G., Hakala, J., Petäjä, T., Mauldin III, R. L., Kulmala, M., and Worsnop, D. R. (2012). Atmospheric Sulphuric Acid and Neutral Cluster Measurements Using CI-Api-TOF. *Atmos. Chem. Phys.*, 12:4117–4125.

Junninen, H., Ehn, M., Petäjä, T., Luosujärvi, L., Kotiaho, T., Kostiainen, R., Rohner, U., Gonin, M., Fuhrer, K., Kulmala, M., and Worsnop, D. R. (2010). A High-Resolution Mass Spectrometer to Measure Atmospheric Ion Composition. *Atmos. Meas. Tech.*, 3:1039–1053.

Kangasluoma, J., Attoui, M., Korhonen, F., Ahonen, L., Siivola, E., and Petäjä, T. (2016a). Characterization of a Herrmann-Type High-Resolution Differential Mobility Analyzer. *Aerosol Sci. Technol.*, 50(3):222–229. doi:10.1080/02786826.2016.1142065.

Kangasluoma, J., Franchin, A., Duplissy, J., Ahonen, L., Korhonen, F., Attoui, M., Mikkilä, J., Lehtipalo, K., Vanhanen, J., Kulmala, M., and Petäjä, T. (2015). Operation of the Airmodus A11 Nano Condensation Nucleus Counter at Various Inlet Pressures, Various Operation Temperatures and Design of a New Inlet System. *Atmos. Meas. Tech. Discuss.*, 8(8):8483–8508. doi:10.5194/amtd-8-8483-2015.

Kangasluoma, J., Junninen, H., Lehtipalo, J., Mikkila, J., Vanhanen, J., Attoui, M., Sipila, M., Worsnop, D. R., Kulmala, M., and Petäjä, T. (2013). Remarks on Ion Generation for CPC Detection Efficiency Studies in Sub-3-Nm Size Range. *Aerosol Sci. Technol.*, 47(5):556–563. doi:10.1080/02786826.2013.773393.

Kangasluoma, J., Kuang, C., Wimmer, D., Rissanen, M. P., Lehtipalo, K., Ehn, M., Worsnop, D. R., Wang, J., Kulmala, M., and Petäjä, T. (2014). Sub-3 Nm Particle Size and Composition Dependent Response of a Nano-CPC Battery. *Atmos. Meas. Tech.*, 7(3):689–700. doi:10.5194/amt-7-689-2014.

Kangasluoma, J., Samodurov, A., Attoui, M., Franchin, A., Junninen, H., Korhonen, F., Kurtén, T., Vehkamäki, H., Sipilä, M., Lehtipalo, K., Worsnop, D. R., Petäjä, T., and Kulmala, M. (2016b). Heterogeneous Nucleation Onto Ions and Neutralized Ions - Insights Into Sign-Preference. *J. Phys. Chem. C*, 120:7444–7450. doi:10.1021/acs.jpcc.6b01779.

Kazil, J., Stier, P., Zhang, K., Quaas, J., Kinne, S., O'Donnell, D., Rast, S., Esch, M., Ferrachat, S., Lohmann, U., and Feichter, J. (2010). Aerosol Nucleation and Its Role for Clouds and Earth's Radiative Forcing in the Aerosol-Climate Model ECHAM5-HAM. *Atmos. Chem. Phys.*, 10:10733–10752. doi:10.5194/acp-10-10733-2010, 2010.

Ku, B. K., and Fernández de la Mora, J. (2004). Cluster Ion Formation in Electrosprays of Acetonitrile Seeded with Ionic Liquids. *J. Phys. Chem. B.*, 108:14915–14923.

Kuang, C., Chen, M., McMurry, P. H., and Wang, J. (2012). Modification of Laminar Flow Ultrafine Condensation Particle Counters for the Enhanced Detection of 1 nm Condensation Nuclei. *Aerosol Sci. Technol.*, 46:309–315.

Kulmala, M., Kontkanen, J., Junninen, H., Lehtipalo, K., Manninen, H. E., Nieminen T., Petäjä, T., Sipilä, M., Schobesberger, S., Rantala, P., Franchin, A., Jokinen, T., Järvinen, E., Äijälä, M., Kangasluoma, J., Hakala, J., Aalto, P. P., Paasonen, P., Mikkilä, J., Vanhanen, J., Aalto, J., Hakola, H., Makkonen, U., Ruuskanen T., Mauldin, III, R. L., Duplissy, J., Vehkamäki, H., Bäcj, J., Kortelainen, A., Riipinen, I., Kurtén, T., Johnston, M. V., Smith, J. N., Kerminen, V-M., and Worsnop, D. R. (2013). Direct Observations of Atmospheric Aerosol Nucleation. *Science*, 339:943–946.

Kulmala, M., Riipinen, I., Sipilä, M., Manninen, H. E., Petäjä, T., Junninen, H., Dal Maso, M., Mordas, G., Mirme, A., Vana, M., Hirsikko, A., Laakso, L., Harrison, R., Hanson, I., Leung, C., Lehtinen, K. E. J., and Kerminen, V.-M. (2007). Toward Direct Measurement of Atmospheric Nucleation. *Science*, 318(5847):89–92.

Larriba, C., and Hogan, C. J. (2013). Free Molecular Collision Cross Section Calculation Methods for Nanoparticles and Complex Ions with Energy Accommodation. *J. Comput. Phys.*, 251:344–363.

Larriba, C., Hogan, C. J., Attoui, M., Borrajo, R., Fernández Garcia, J., and Fernández de la Mora, J. (2011). The Mobility-Volume Relationship below 3.0nm Examined by Tandem Mobility-Mass Measurement. *Aerosol Sci. Technol.*, 45(4):453–467.

López-Yglesias, X., and Flagan, R. C. (2013). Ion–Aerosol Flux Coefficients and the Steady-State Charge Distribution of Aerosols in a Bipolar Ion Environment. *Aerosol Sci. Technol.* 47:688–704.

Maisser, A., Thomas, J. M., Larriba-Andaluz, C., He, S., and Hogan, C. J. (2015). The Mass-Mobility Distributions of Ions Produced by a Po-210 Source in Air. *J. Aerosol. Sci.* 90:36–50.

Manninen, H. E., Nieminen, T., Asmi, E., Gagné, S., Häkkinen, S., Lehtipalo, K., Aalto, P., Vana, M., Mirme, A., Mirme, S., Hõrrak, U., Plass-Dülmer, C., Stange, G., Kiss, G., Hoffer, A., Törő, N., Moerman, M., Henzing, B., de Leeuw, G., Brinkenberg, M., Kouvarakis, G. N., Bougiatioti, A., Mihalopoulos, N., O'Dowd, C., Ceburnis, D., Arneth, A., Svenningsson, B., Swietlicki, E., Tarozzi, L., Decesari, S., Facchini, M.C., Birmili, W., Sonntag, A., Wiedensohler, A., Boulon, J., Sellegri, K., Laj, P., Gysel, M., Bukowiecki, N., Weingartner, E., Wehrle, G., Laaksonen, A., Hamed, A., Joutsensaari, J., Petäjä, T., Kerminen, V.-M., and Kulmala, M. (2010). EUCAARI Ion Spectrometer Measurements at 12 European Sites – Analysis of New Particle Formation Events. *Atmos. Chem. Phys.*, 10(16):7907–7927. doi:10.5194/acp-10-7907-2010.

Martínez-Lozano, P., and Fernández de la Mora, J. (2005). Effect of Acoustic Radiation on DMA Resolution. *Aerosol Sci. Technol.*, 39(9):866–870.

Merikanto, J., Spracklen, D. V., Mann, G. W., Pickering, S. J., and Carslaw, K. S., (2009). Impact of Nucleation on Global CCN. *Atmos. Chem. Phys.*, 9:8601–8616. doi:10.5194/acp-9-8601-2009.

Mesleh, M. F., Hunter, J. M., Shvartsburg, A. A., Schatz, G. C., and Jarrold, M. F. (1996). Structural Information from Ion Mobility Measurements: Effects of the Long-Range Potential. *J. Phys. Chem.*, 100:16082–16086.

Rosell-Llompart, J., and Fernández de la Mora, J. (1994). Generation of Monodisperse Droplets 0.3 to 4μm in Diameter From Electrified Cone-Jets of Highly Conducting and Viscous Liquids. *J. Aerosol Sci.*, 26(6):1093–1119.

Rosell-Llompart, J., Loscertales, I. G., Bingham, D., and Fernández de la Mora, J., (1996). Sizing Nanoparticles and Ions with a Short Differential Mobility Analyzer. *J. Aerosol Sci.*, 27(5):695–719. doi:10.1016/0021-8502(96)00016-X.

Shvartsburg, A. A., Mashkevich, S. V., Baker, E. S., and Smith, R. D. (2007). Optimization of Algorithms for ion Mobility Calculations. *J. Phys. Chem. A*, 111:2002–2010.

Steiner, G., Attoui, M., Wimmer, D., and Reischl, G. P. (2010). A Medium Flow, High-Resolution Vienna DMA running in Recirculating Mode. *Aerosol Sci. Technol.*, 44(4):308–315.

Steiner, G., Jokinen, T, Junninen, H, Sipilä, M., Petäjä, T., Worsnop, D. R., Reischl, G. P., and Kulmala, M. (2014). High-Resolution Mobility and Mass Spectrometry of Negative Ions Produced in an ^{241}Am Aerosol Charger. *Aerosol Sci. Technol.*, 48(3):261–270.

Steiner, G., and Reischl, G. P. (2012). The Effect of Carrier Gas Contaminants on the Charging Probability of Aerosols Under Bipolar Charging Conditions. *J. Aerosol Sci.*, 54:21–31.

Stolzenburg, M. R., and McMurry, P. H. (1991). An Ultrafine Aerosol Condensation Nucleus Counter. *Aerosol. Sci. Technol.*, 14(1):48–65.

Tammet, H. (1995). Size and Mobility of Nanometer Particles, Clusters and Ions. *J. Aerosol. Sci.*, 26(3):459–475.

Ude, S., and Ferández de la Mora, J. (2005). Molecular Monodisperse Mobility and Mass Standards from Electrosprays of Tetra-Alkyl Ammonium Halides. *J. Aerosol Sci.*, 36:1224–1237.

Vanhanen, J., Mikkilä, J., Lehtipalo, K., Sipilä, M., Manninen, E., Siivola, E., Petäjä, T., and Kulmala, M. (2011). Particle Size Magnifier for Nano-CN Detection. *Aerosol Sci. Technol.*, 45(4):533–542.

Winkler, P. M., Steiner, G., Vrtala, A., Vehkamäki, H., Noppel, M., Lehtinen, K. E. J, Reischl, G. P., Wagner, P. E., and Kulmala, M. (2008). Heterogeneous Nucleation Experiments Bridging the Scale from Molecular Ion Clusters to Nanoparticles. *Science*, 319:1374–1377.